Use of biopolymers as oriented supports for the stabilization of different polymorphs of biomineralized calcium carbonate with complex shape

Mario Díaz-Dosque [a,f], Pilar Aranda [b], Margarita Darder [b], Jaime Retuert [c,f,1], Mehrdad Yazdani-Pedram [e,f], José Luis Arias [d,f], Eduardo Ruiz-Hitzky [b,*]

[a] Facultad de Odontología, Universidad de Chile, Chile
[b] Instituto de Ciencia de Materiales de Madrid, CSIC, Cantoblanco, 28049 Madrid, Spain
[c] Facultad de Ciencias Físicas y Matemáticas, Universidad de Chile, Chile
[d] Facultad de Veterinaria y Ciencias Animales, Universidad de Chile, Chile
[e] Facultad de Ciencias Químicas y Farmacéuticas, Universidad de Chile, Chile
[f] Centro para la Investigación Interdisciplinaria Avanzada en Ciencias de los Materiales (CIMAT), Chile

A B S T R A C T

This work concerns the use of different biopolymers such as chitosan, alginate or κ-carrageenan as substrates to contribute to the study of the crystallization of calcium carbonate. The experimental biomimetic approach involves the preparation of mixtures of biopolymer solutions with a solution of $CaCl_2$, which is processed by means of spin-coating and then exposed to CO_2 by a slow diffusion method for the growth of $CaCO_3$. The obtained crystals show that each biopolymer has different effects on the crystallization habit. Different agglomerations of calcium carbonate crystals are initially the vaterite phase, which is subsequently stabilized as calcite. Biomineralization on each biopolymer gave rise to complex structures very different to those normally found *in vitro,* but similar to those observed in Nature. This confirms the strong influence of the macromolecules with ionizable groups on the stabilization of a determined polymorph and also on the morphology of the calcium carbonate crystals.

Keywords:
A1. Biomineralization
B1. Calcite
B1. Vaterite
B1. Biopolymers
B1. Chitosan
B1. Carrageenan

1. Introduction

The process known as biomineralization is the process leading to the formation of a variety of solid inorganic structures by living organisms, such as prokaryotes intracellular crystals, protozooan, invertebrate exoskeletons, bone, teeth, eggshells and oyster pearls [1–4]. Many organisms in the nature produce materials based on calcium carbonate with complex forms and novel properties. It is known that calcium carbonate may crystallize into three different polymorphs: calcite, the rhombohedral polymorph that is the most thermodynamically stable form, followed in stability by aragonite, which is orthorhombic and vaterite, the hexagonal form that is the less stable phase and is synthesized by direct precipitation [5,6].

The crystallization process *in vivo* is a complex process. There are many possible pathways in the particle-formation process, such as nanospherulites aggregation-induced crystallization or transformation by simple crystal growth. The existence of several phases would enable an organism to control kinetically the mineralization process. By selectively interacting with the mineral at different stages during the crystal-forming process, the organism may choose to manipulate both the polymorph and the orientation of the mineral to meet specific biological requirements [7].

Traditional synthetic routes to modifying the morphology rely upon manipulation of such variables as supersaturation, reactant flow rates, temperature and pressure. Inorganic and organic additives are also widely employed to afford relatively simple changes in single crystal morphologies [8–11]. More significant changes in morphology can be attributed to a change from single

* Corresponding author. Fax: +34 91 3720623.
E-mail address: eduardo@icmm.csic.es (E. Ruiz-Hitzky).
[1] Deceased.

crystal to polycrystalline structure [11–15]. Interaction of an additive with a specific set of crystal planes results in stabilization of these planes, their expression in the final form of the crystal and, therefore, in the modification of the morphology. There is significant evidence that organisms use macromolecules to control crystal growth, orientation and morphology [16,17].

Therefore, *in vitro* study of crystallization of calcium carbonate could be carried out in a biomimetic way by using biopolymers. These polymers could control crystal growth, habit and morphology through molecular interactions at the nanoscale [18–21]. Biopolymers can also adsorb onto crystal surfaces, altering the stability of that face and hence affecting the growth rate. These organic regulators are often identified as polymers with different functional groups [22].

In a classic example such as the mollusk shells, the inorganic components are dominant with over 95% of the mass or volume. Those in the prismatic layer are (0 0 1)-oriented calcite crystals, and those in the nacreous layer are *c*-axis-oriented aragonite tablets [23]. The organic matrix is composed of *β*-chitin, silk-fibroin-like proteins, and acidic macromolecules in the interlamellar space between crystals [24].

Biopolymers are provided with different functional groups. In the case of alginate, it is a natural block copolymer extracted from seaweeds, composed of linear unbranched polymers containing β-(1→4)-linked D-mannuronic acid and α-(1→4)-linked L-guluronic acid (Fig. 1a). κ-carrageenan, (1→3)-β-D-galactopyranose-4-sulfate-(1→4)-3,6-anhydro-α-D-galactopyranose-(1→3), is a functional biopolymer also extracted from the seaweed but, in this case, it contains sulfate groups (Fig. 1b). On the other hand, chitosan (poly-*β*-(1→4)-2-amino-2-deoxy-D-glucose) obtained through partial deacetylation of chitin (poly-*β*(1→4)-2-acetamido-2-deoxy-D-glucose) is the only pseudo-natural cationic polymer (Fig. 1c) [25]. Despite their importance in the field of biomineralization, where anionic polysaccharides provide the template for the intricate hierarchical assemblies of calcium carbonate crystals in coccoliths [26,27], relatively little work has been done on the systematic study of the influence of simple polysaccharides on calcium carbonate crystallization. The presence of the different polymorphs was explained by the differences in geometrical matching and stereochemical complementarity between the calcium ions and the different groups on the biopolymers.

An understanding of the mechanism involved in such a matrix-mediated synthesis has been recognized to be of great potential in the production of engineered materials following biomimetic approaches.

In this work, the influence of different biopolymers on *in vitro* crystallization of calcium carbonate was studied. These

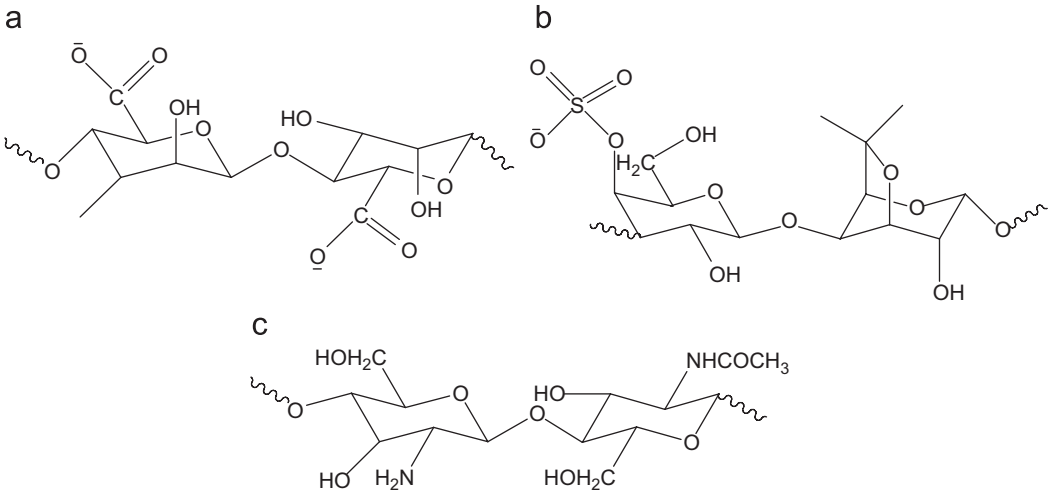

Fig. 1. Structures of alginate (a), κ-carrageenan (b) and chitosan (c).

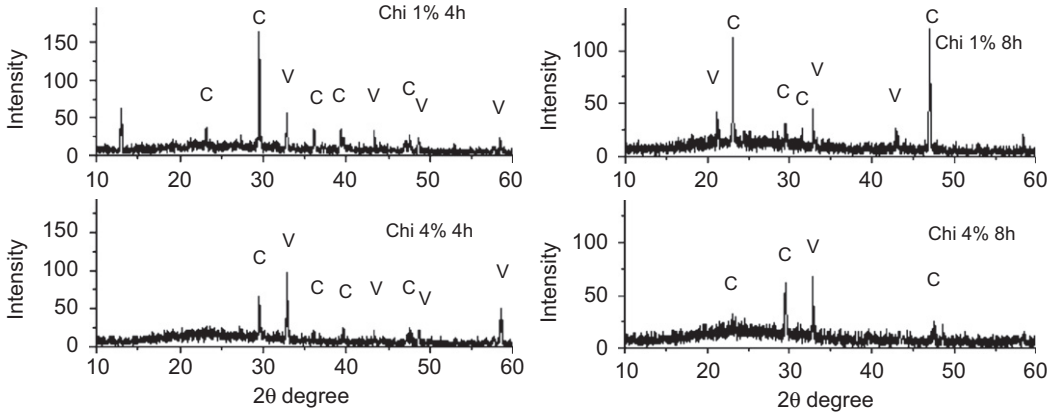

Fig. 2. XRD patterns of mineralized chitosan (Chi) films prepared from 1% and 4% chitosan solutions, exposed to CO_2 for 4 and 8 h.

biopolymers that, in general, show high affinity for Ca^{2+} ions were selected in order to observe the effects of calcium binding, number and type of side groups, i.e. carboxylate and sulfate, on the resulting calcium carbonate morphology and polymorphs. In addition, the biopolymer matrices were prepared as oriented supports under spin-coating conditions. Biomineralized materials such as shells found in living organisms show in most of the cases a well-defined orientation. As previously reported [28], hydrogels formed under dynamic conditions resulted in ordered scaffolds that promote uniform distribution of transplanted cells. Falini et al. [29] also reported the oriented deposition of vaterite in cross-linked gelatin films, where the ordered and oriented polypeptide chains can contribute to the control of polymorphism. In a similar way, it is expected that the orientation imposed by the spin-coating process to the polysaccharide matrices in the present study may also have a strong influence on the $CaCO_3$ growth.

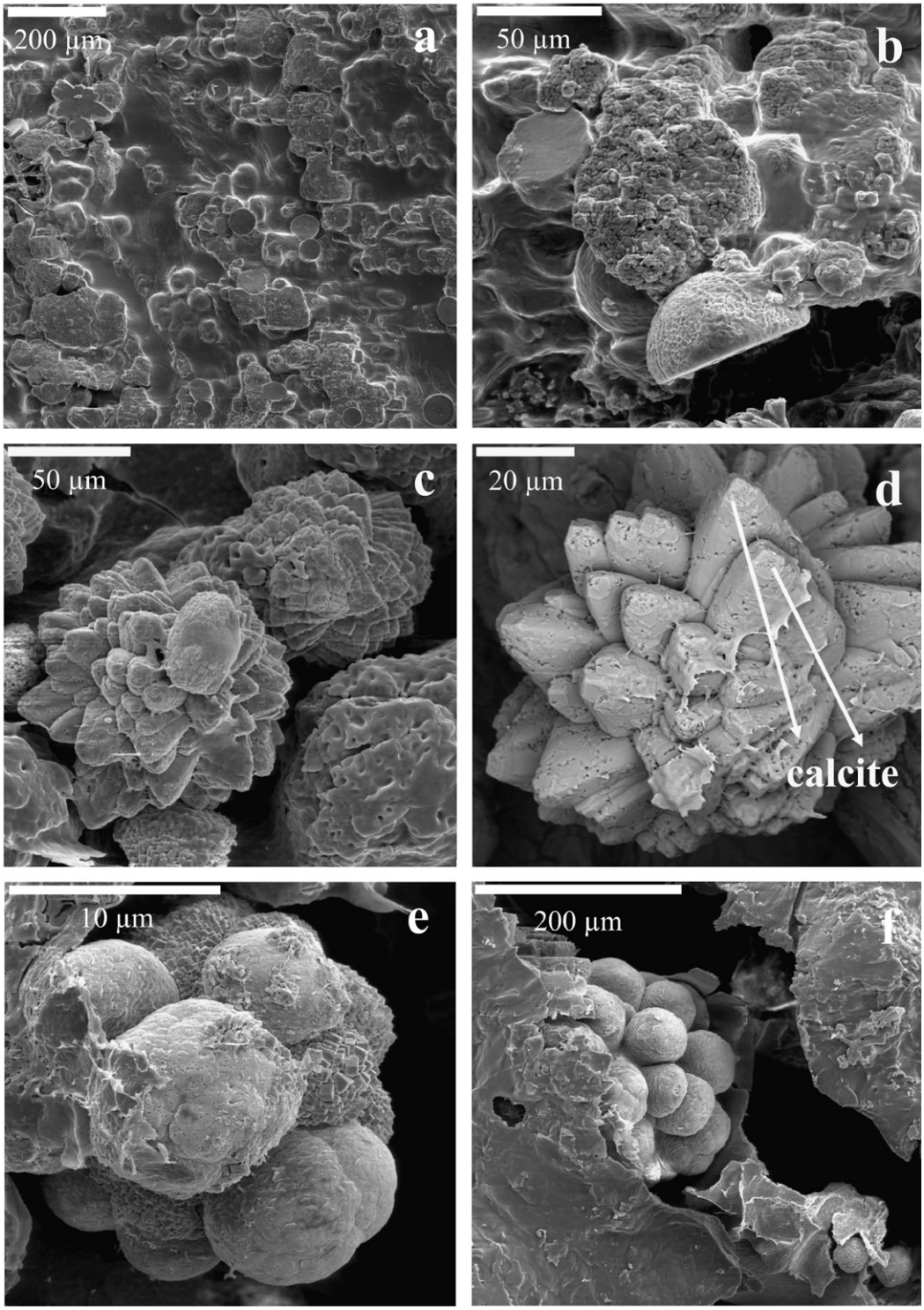

Fig. 3. SEM micrographs of $CaCO_3$ crystals obtained on films prepared from 1% chitosan after different periods of exposition to CO_2: (a) and (b) 4 h; (c) and (d) 8 h; (e) and (f) 24 h.

2. Experimental procedure

2.1. Materials

Chitosan sample of high molecular weight (Mw = 350 KDa) with 83.5% deacetylation from Aldrich was purified by dissolution in dilute acetic acid, filtered to remove insoluble fraction and unwanted solids and then was lyophilized.

Dehydrated calcium chloride, ethanol and tris(hydroxymethyl)-aminomethane were obtained from Merck and ammonium hydrogen carbonate was from J.T. Baker. These reagents were of the highest available grade and used without further purification. Alginic acid sodium salt and κ-carrageenan were purchased from Aldrich and were used as received (Alginate %M = 60, %G = 40, %MM = 40, %GG = 40, M/G = 1.5; κ-carrageenan with 3.2 mmol–OSO_3^-/g biopolymer, as deduced from CHNS Chemical Analysis, as well as an experimental charge/dimer ratio of 1.03 [30]).

2.2. Methods

Films of different biopolymers to be used as substrate for the calcium carbonate crystallization were prepared by spin-coating. First, solutions of biopolymers, either 1% or 4% by weight, were prepared. To a small Petri-dish 2 ml of each biopolymer solution was added. The Petri-dish containing the biopolymer solution was placed in the spin-coating apparatus (Single Wafer Spin Processor, model WS-400A-6 NPP/LITE SHOWN, from Laurell Technologies Corporation, North Wales, PA) and the biopolymer film was cast at 500 rpm for 2 min by adding, drop wise, 2 ml of solution of 1 M calcium chloride in Tris buffer at pH 9. Mineralization experiments were carried out in the presence of the biopolymer film samples, as structure-directing substrates, by using the slow CO_2 diffusion method [31,32]. This method is based on the generation of CO_2 by slow decomposition of ammonium hydrogencarbonate. The crystallization experiments were carried out for periods of 1, 2, 4, 6, 8, 24 and 48 h, where films of chitosan, alginate or κ-carrageenan were placed inside of a polystyrene microbridge in the chamber. Precipitation of $CaCO_3$ results from the diffusion of carbon dioxide vapor into the buffered $CaCl_2$ solution. The polymeric substrates with the crystals of the different polymorphs of $CaCO_3$ formed were collected. Once rinsed with distilled water and with 50–100% gradient ethanol solutions, they were dried at room temperature and finally coated with gold using an EMS-550 automated sputter coater. The crystals were observed in a Zeiss DSM 960 scanning electron microscope (SEM). The X-ray diffraction (XRD) patterns were taken from powdered samples using a Bruker D8 X-ray diffractometer with CuK_α radiation.

3. Results and discussion

3.1. Chitosan as oriented support for calcium carbonate growth

In a previous work, we have studied the use of chitosan biopolymer in the gel form for calcium carbonate growth, observing that only rhombohedral calcite was obtained independent from mineralization time and mineralization conditions used [33]. Now we have introduced a new experimental approach in which the biopolymer is used as an oriented support processed by spin-coating following the methodology described in the Section 2. The application of this methodology allows to prepare films of chitosan, from either 1% or 4% solutions of this biopolymer, leading to the presence of vaterite and calcite after 4 h of mineralization. XRD diagrams show peaks at $2\theta = 27.1^\circ$, $2\theta = 32.7^\circ$, $2\theta = 50.1^\circ$ and $2\theta = 58.5^\circ$ corresponding to the (1 3 2), (0 2 4), (2 2 2) and (1 1 5) planes of vaterite, as well as peaks at $2\theta = 29.5^\circ$, $2\theta = 36.1^\circ$, $2\theta = 47.6^\circ$ and $2\theta = 48.6^\circ$ assigned to (1 0 4), (1 1 0), (0 2 4) and (0 1 8) planes of calcite (Fig. 2). After 8 h of reaction, still both calcite and vaterite are present, although for the films containing 1% of chitosan an increase in the intensity of diffraction peaks at $2\theta = 47.6^\circ$ and $2\theta = 23.1^\circ$ corresponding to the (0 2 4) and (0 1 2) planes of calcite is observed. To explain the templating action of chitosan in the preferential growth of calcite polymorph with the (0 2 4) and the (0 1 2) planes of higher intensity than the other ones, e.g. the (1 0 4) plane, the tendency of this biopolymer to arrange itself in layers could be taken into account. The ability of chitosan layers in the organization of silica and silica-derivatives generated from silicon alkoxides in the presence of this biopolymer has been reported [34]. The use of spin-coating for the preparation of the support may accentuate this effect of preferential orientation of chitosan and, therefore, of the preferential oriented growth of calcite in contrast to bulk chitosan prepared without spin-coating processing [33].

In a similar way to what occurs with other biopolymers, it is also observed here that polymorphs vaterite and calcite are formed and stabilized independently from the mineralization time. However, more vaterite is formed and stabilized when films with higher amount of chitosan are used as oriented support.

The morphology of the calcium carbonate crystals obtained by using chitosan oriented films is shown in Fig. 3. After 4 h of treatment two different arrangements of crystals are formed. One of them is visualized as planar semi-circles that could be vaterite, and the other one results in an agglomeration of calcite crystals (Fig. 3a) of around 2 μm (Fig. 3b). After 8 h of treatment, spherical structures consisting of agglomeration of prismatic calcite crystals on their surfaces are observed (Fig. 3c). Also, lamellar agglomerates of crystals are obtained with a morphology resembling flowers, where calcite crystals can be recognized on the extreme of their petals (Fig. 3d) [35]. The growth of these crystal-petals occurs following a helical arrangement that can be the reason why the intensities of the diffraction peaks corresponding to the (0 1 2) and (0 2 4) planes increase in the XRD pattern shown in Fig. 2b. In general, calcite crystal growth occurs preferentially in the direction of the plane (1 0 4). In contrast, the oriented growth observed here could be due to a local arrangement of the functional groups of chitosan, which may act as preferential centers for the calcite growth. It can be postulated that in this situation the development of (0 1 2) and (0 2 4) calcite planes is

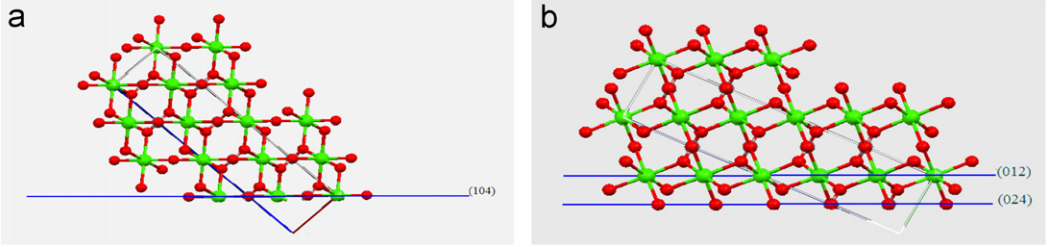

Fig. 4. View of the calcite structure from different orientations: (a) in the plane (1 0 4), and (b) in the plane (0 1 2). Red: oxygen; green: calcium.

favored, in which calcium and oxygen are arranged in layers within the unit cell (Fig. 4).

After 24 h of treatment, two types of spherical structures are observed, one with smooth surface and the other one with prismatic calcite crystals whose size is around 5 μm (Figs. 3e and f).

Films prepared from 4% chitosan produce spherical structures with smooth surfaces and also agglomerates of calcite crystals (both indicated by arrows in Fig. 5). The coexistence of apparently amorphous calcium carbonate and calcite crystals could be associated with the higher concentration and viscosity of the chitosan solution employed in the film preparation. This high viscosity may also affect the evolution of initially formed amorphous calcium carbonate to other more stable polymorphs.

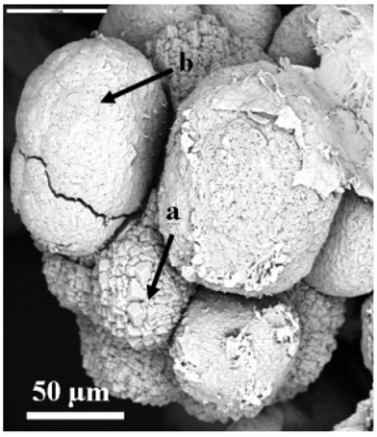

Fig. 5. SEM micrograph of $CaCO_3$ crystals obtained by using films prepared from 4% chitosan after 24 h of exposition to CO_2.

3.2. Alginate as oriented support for calcium carbonate growth

XRD and SEM analyses were used to study the nature of the polymorphs as well as the morphology of calcium carbonate crystals, respectively. The XRD patterns of mineralized film samples prepared from either 1% or 4% of alginate, as a function of the mineralization time, are shown in Fig. 6. As seen in these graphs, diffraction at $2\theta = 31.8^\circ$ corresponding to calcium chloride disappears after 2 h of mineralization and new signals at $2\theta = 29.5^\circ$ and $2\theta = 32.7^\circ$ appear. The first peak corresponds to the (1 0 4) plane of calcite and the second one to the (0 2 4) plane of vaterite. The relative intensity of both signals increases by increasing the mineralization time, but after 4 h a signal at $2\theta = 23^\circ$ associated with the (0 1 2) plane of calcite is clearly observed. Although the same signals are observed for both alginate concentrations, the film with higher amount of alginate shows more intense signals. No significant variation in the relative intensity of diffraction peaks of calcite to vaterite was observed after 24 h of mineralization (XRD not shown).

The morphology of calcium carbonate crystals was observed by SEM. Fig. 7a shows the formation of vaterite crystals of spherical shape (ca. 5 μm diameter) as well as flower-shaped crystals [31] when films containing 1% alginate were exposed to CO_2 for 4 h. After 6 h of treatment, agglomerates of the same crystal type mimicking sponge were obtained (Fig. 7b).

When films of 4% alginate were used, after 1 h some crystals surrounding a hemispherical nucleus were formed. These could be crystals of calcium chloride as revealed by XRD. However, it is possible to observe as concentric circumferences the presence of bulky shells surrounding the internal cavity inside these hemispheres (Fig. 7c). Also prismatic type crystals of approximately 100 nm are observed on the surface of these hemispheres. After 4 h of exposure to CO_2, crystal growth around these nuclei was continued maintaining the inner cavity, giving as a result, columns of vaterite crystals of 1–2 μm (Fig. 7d). In some cases,

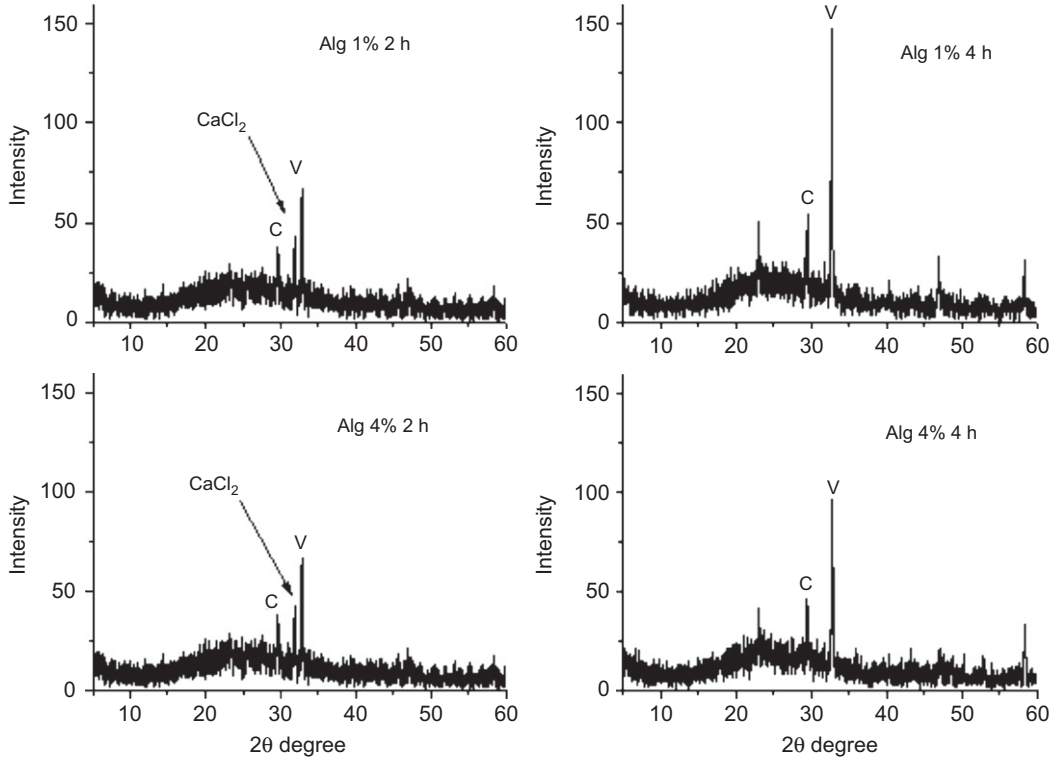

Fig. 6. XRD patterns of mineralized alginate (Alg) films prepared from different biopolymer concentration (1% and 4%) after exposure to CO_2 for 2 and 4 h. (C: calcite; V: vaterite).

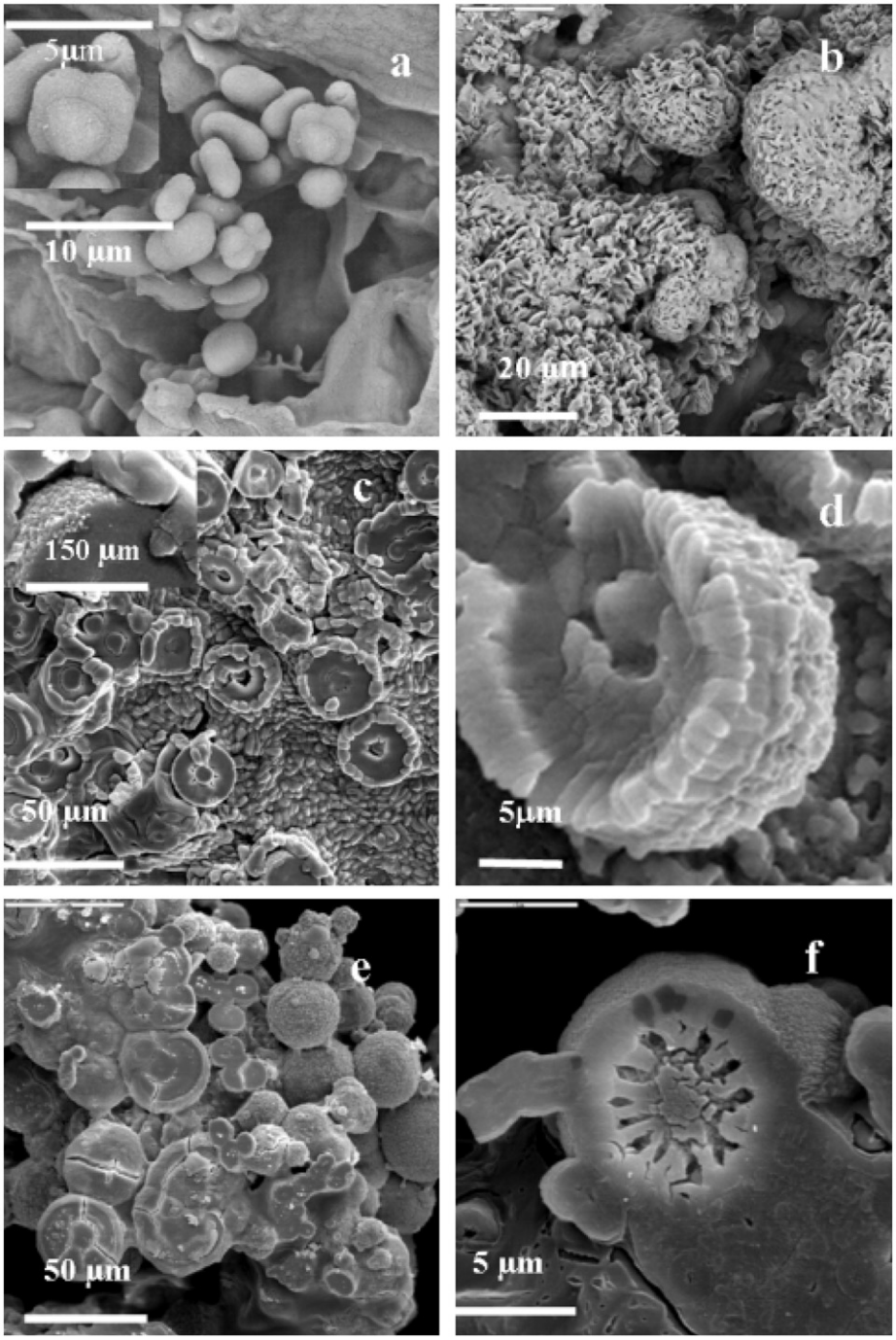

Fig. 7. SEM images of $CaCO_3$ produced by exposure of alginate films, containing either 1% or 4% of alginate, to CO_2 atmosphere for different periods of time: (a) 1% 4 h, (b) 1% 6 h, (c) 4% 1 h, (d) 4% 4 h, (e) 4% 6 h, and (f) 4% 24 h. Insets in (a) and (c) correspond to magnified crystals.

after 6 h of mineralization, these columns were transformed to spherical structures surrounded by prismatic calcite crystals of less than 150 nm length, although hemispherical structures are still present (Fig. 7e).

After 24 h of reaction, almost all structures are spherical consisting of calcite crystals ($<$150 nm) covering the surface. Moreover, it is still possible to distinguish hemispherical crystals with the cavity located at the particle center, from which a radial arrangement is observed (Fig. 7f). Fractures in the larger hemispheres are also observed, probably due to a phenomenon of volume reduction as consequence of solid–solid transitions of calcium carbonate polymorphs, from amorphous to vaterite and/or from vaterite to calcite [32]. In order to explain this volume reduction, it can be considered that amorphous calcium carbonate contains 1.0–1.5 water molecules per each calcium carbonate unit, which could be eliminated in these transitions [36]. On the other hand, the density of calcite and vaterite is approximately 2.71 and 2.45, respectively, and the transition of vaterite to calcite may involve a volume reduction of 6.3% [32]. Therefore, the generation of these fractures could most likely be due to the transition from vaterite to calcite. This last interpretation has been further confirmed by XRD analysis, which shows the presence of both crystalline phases coexisting in these samples. Hence, it should be postulated that the initial phase formed was amorphous calcium

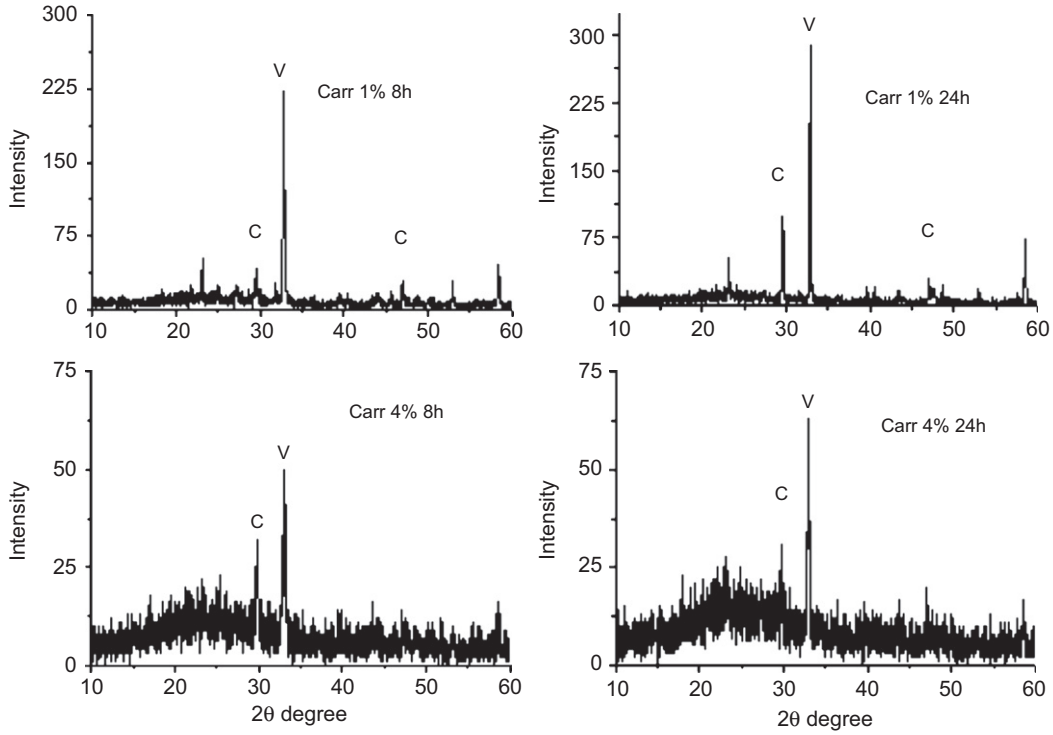

Fig. 8. XRD patterns of mineralized κ-carrageenan (Carr) films, prepared from 1% and 4% κ- carrageenan solutions, exposed to CO_2 during different periods of time.

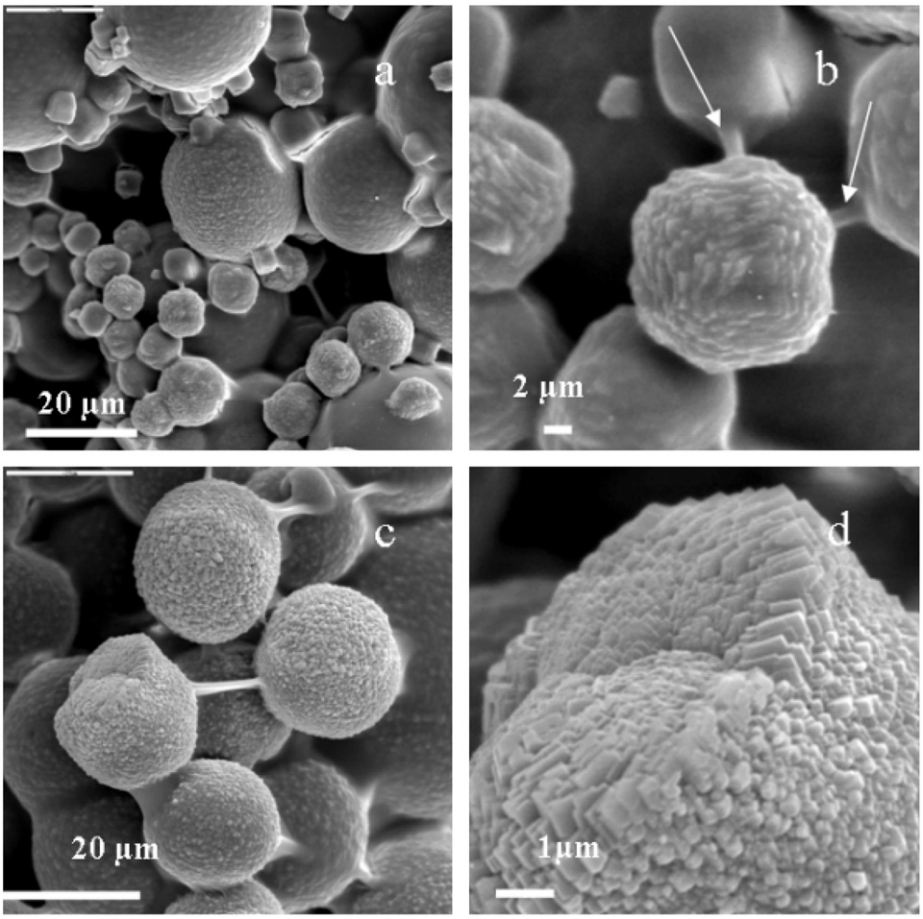

Fig. 9. SEM micrographs of $CaCO_3$ crystals on films prepared from 1% κ-carrageenan after different periods of exposure to CO_2: (a) 6 h; (b) magnification of (a); (c) 24 h; and (d) magnification of (c).

carbonate with subsequent transition from vaterite to calcite. The morphology of some structures observed in Fig. 7 could be considered as mimetic of those biomineralized by the *Porcellio scaber* organisms [37].

3.3. κ-Carrageenan as oriented support for calcium carbonate growth

Following a similar approach, κ-carrageenan films processed by spin-coating were also used as a support for calcium carbonate growth. In this case, after 8 h of exposition of κ-carrageenan films (prepared from 1% and 4% biopolymer solutions) to CO_2, three characteristic signals are observed in the XRD patterns of the mineralized samples at 29.5°, 31.8° and 32.7° 2θ, respectively (Fig. 8). The first diffraction peak is assigned to the (1 0 4) plane of calcite, the second signal belongs to calcium chloride and the third one to the (0 2 4) plane of vaterite. By increasing the exposure time to 24 h, the peak corresponding to calcium chloride disappears and new signals appear at $2\theta = 47.1°$ and at $2\theta = 58.5°$, which can be attributed to the (0 2 4) and to (1 1 5) planes of calcite and vaterite, respectively. The intensities of all the XRD peaks increase by increasing the mineralization time, being most significant the increase of the signal associated with

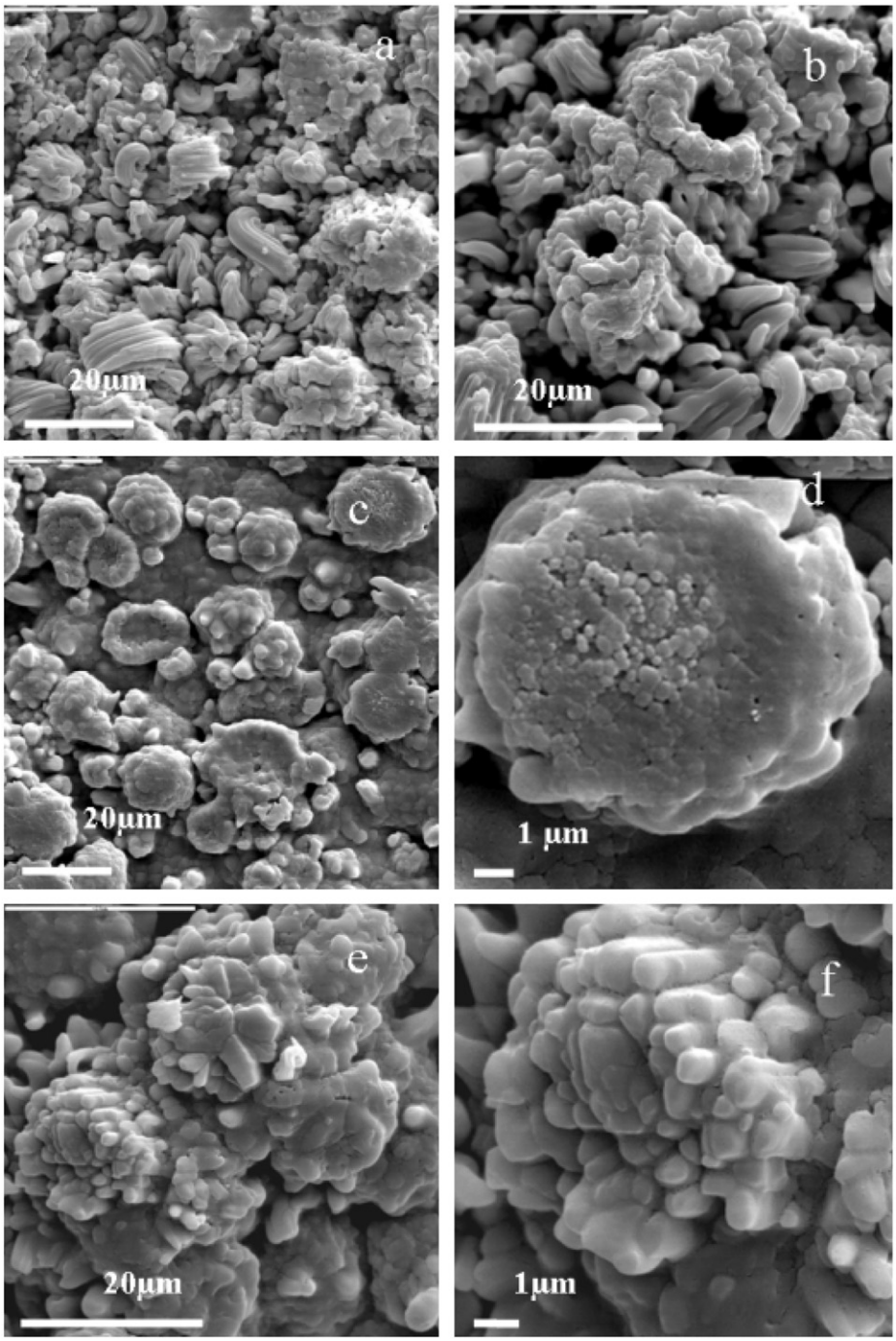

Fig. 10. SEM micrographs of $CaCO_3$ crystals grown on films prepared from 4% κ-carrageenan, after different periods of exposure to CO_2: (a) and (b) 4 h; (c) and (d) 6 h; (e) and (f) 8 h.

vaterite. This behavior is similar to the process occurring in Nature, where the metastable polymorphs of calcium carbonate (i.e. vaterite) can be stabilized by living organisms [38].

The above features could be tentatively explained by considering that the large number of sulfate groups on κ-carrageenan could generate non-homogenously distributed local charges. It could be invoked that differences in the local charge on the biopolymer films could produce a local Ca^{2+} supersaturation. Therefore, the interaction of the biopolymer with calcium ions could lead to the direct nucleation, growth and stabilization of different polymorphs of calcium carbonate on the polymer surface. SEM studies (Fig. 9) show that both vaterite as well as calcite are formed under the experimental conditions used in this work and that the polymorph of vaterite is actually stabilized. Moreover, this polymorph predominates over the calcite, which is the most stable polymorph of $CaCO_3$.

SEM images show the presence of agglomerates of crystals with spherical morphology (ca. 20 μm diameter) on the mineralized films prepared from 1% κ-carrageenan and exposed to CO_2 for 6 h (Fig. 9a). Besides, smaller and less spherical agglomerates of crystals, probably polyhedral calcite, are also present (Fig. 9b). It is also observed in this last figure the presence of crystals bridging the agglomerates (arrows in Fig. 6b), which could be due to the polymorph vaterite surrounded by calcite crystals, in agreement with XRD patterns. These agglomerates are completely transformed into spherical structures of approximately 30 μm diameter after 24 h of reaction (Fig. 9c). Additionally, in this case some helical arrangements of calcite crystals with nanometric dimensions are observed (Fig. 9d).

When films prepared from 4% κ-carrageenan are used as support, worm-like crystals are obtained after 4 h of exposure to CO_2 (Fig. 10a). Crystals forming a tube-like structure and showing dimensions ranging from 300 nm to 2 μm are also observed in other zones of the same sample (Fig. 10b). After 6 h, agglomerates of $CaCO_3$ crystals of 2 μm similar to a jigsaw puzzle are formed (Fig. 10c). The magnification of one of these structures shows the presence of crystals (ca. 125 nm size) as seeds initiating their formation (Fig. 10d). However, after 8 h a column type crystal growth is observed instead (Figs. 10e and f).

In experiments involving films prepared from 1% κ-carrageenan, calcite crystals were formed in some cases, while vaterite was obtained by increasing the amount of κ-carrageenan to 4%. As above invoked, the possible explanation for this behavior could be ascribed to the increase of Ca^{2+} ions adsorbed on the biopolymer surface producing a supersaturation that favors a fast nucleation and growth of the vaterite polymorph. On the other hand, crystal growth in the form of columns could be due to the local conformation and chain orientation of the biopolymer influencing the crystal orientation and the nature of the $CaCO_3$ polymorph crystals. It could be admitted that the helical conformation adopted by κ-carrageenan in the presence of calcium ions affects the orientation of crystal growth and crystallographic planes leading to those planes being preferentially oriented in a special manner with respect to the substrate film (Fig. 9d). In fact, it has been demonstrated that the amount and distribution of sulfate groups in a polymer differentially modify crystalline morphology [39]. In addition, functionalized self-assembled monolayers with sulfate groups were more active than other negatively charged groups in inducing calcium carbonate nucleation, and the sulfate groups induced a face-selective nucleation [40–42]. Calcium carbonate crystallization on solid functionalized substrates depends on the spacing, ordering and orientation of the terminal group. This could explain the different morphologies induced by the biopolymers used here. Also, this process can occur through the coalescence of primary nanoparticles into colloidal aggregates, often of uniform size, and their subsequent internal restructuration to produce a crystallographically continuous particle of nanometric dimensions (Fig. 10d). Such an aggregation-mediated crystallization appears to be prominent for solids such as copper

Table 1
Summary of the main characteristics observed for the biomineralized $CaCO_3$ grown on biopolymer oriented supports (C: calcite; V: vaterite)

Biopolymer support	Conc. (%w/v)	Biomineralization time (h)	Morphology of observed $CaCO_3$ polymorphs	Conclusions
Chitosan	1	4	Planar semi-circles (V) and agglomerates of C crystals (2 μm)	Preferential growth of C most likely due to the tendency of chitosan to arrange itself in layers
		8	Spherical structures (C) and agglomerates resembling flowers	
		24	Spherical structures (C) with smooth surface and with prismatic C crystals (5 μm)	
	4	24	Spherical structures with smooth surface and agglomerates of C crystals, as well as amorphous calcium carbonate	Presence of amorphous $CaCO_3$. The high viscosity of chitosan may affect its evolution to the more stable polymorphs V and C
Alginate	1	4	Spherical shaped V crystals, 5 μm	As biomineralization time increases, more V is stabilized but C is still observed
		6	Sponge-like V agglomerates	
	4	1	Semi-spheres with an inner cavity and prismatic V crystals (100 nm) in their surface	Transition from initial amorphous $CaCO_3$ to V and finally to C as biomineralization time increases
		4	Semi-spheres comprising columns of V crystals (1–2 μm)	
		6	Spherical structures surrounded by prismatic C crystals (<150 nm length) and semi-spherical structures still observed	
		24	Spherical structures with calcite crystals (<150 μm) covering the surface	
κ-carrageenan	1	6	Spherical agglomerates of V (20 μm) as well as polyhedral C	V predominates but C is still observed
		24	Spherical structures (30 μm)	
	4	4	Worm-like crystals (300 nm–2 μm)	Ca^{2+} supersaturation on biopolymer surface favors fast nucleation and growth of V
		6	Agglomerates of 2 μm crystals similar to a jigsaw puzzle	
		8	Column-type crystals	

oxalate crystallized in the presence of hydroxypropylmethylcellulose (HPMC). The addition of HPMC to the precipitating copper nitrate and sodium oxalate solution induces the self-organization of the crystals, remaining very well aligned crystallographically within the volume of the aggregate [43].

We did not explore the occurrence of the polymers inside the crystals because our experimental approach had to do mainly with a heterogeneous nucleation on the surface of the polymer films. However, we are not able to exclude the possibility that more soluble polymer molecules at the interface could be included inside the crystals, as it has been shown to occur in some biological models [17,44–48].

4. Conclusions

In contrast to previous observations on biomineralization of $CaCO_3$ using chitosan as support where calcite is the only formed polymorph, the application of spin-coating methodologies to orientate the system allows the stabilization of vaterite or calcite depending on the concentration and the biomineralization time (Table 1). This methodology can be also applied to obtain oriented supports of other biopolymers, such as alginate and κ-carrageenan, resulting in the stabilization of different $CaCO_3$ polymorphs (vaterite or calcite) with a great variety of shapes and sizes in the agglomerated crystals. Table 1 summarizes the main features of the biomineralized $CaCO_3$ polymorphs grown on the different studied biopolymer oriented supports.

Acknowledgements

This work has been promoted by the CSIC and the University of Chile (Bilateral project 2006CL0036 and CSIC 04/07-08) and it has been partially supported by CONICYT, Chile (Project: FONDAP 11980002) and the CICYT, Spain (Project: MAT2006-03356). We thank Mr. F. Pinto and Ms. Sara Paniagua for technical assistance in the SEM study. M.D. acknowledges the CSIC for an I3P postdoctoral contract.

References

[1] L. Addadi, S. Weiner, Nature 389 (1997) 912.
[2] B.L. Smith, T.E. Schäffer, M. Viani, J.B. Thompson, N.A. Frederick, J. Kindt, A. Belcher, G.D. Stucky, D.E. Morse, P.K. Hansma, Nature 399 (1999) 761.
[3] S. Mann, G.A. Ozin, Nature 382 (1996) 313.
[4] J.L. Arias, M.S. Fernandez, Mater. Charact. 50 (2003) 189.
[5] J. Küther, R. Seshadri, W. Knoll, W. Tremel, J. Mater. Chem. 8 (1998) 641.
[6] H. Wei, Q. Shen, Y. Zhao, D.-J. Wang, D.-F. Xu, J. Crystal Growth. 250 (2003) 516.
[7] K. Naka, S.-C. Huang, Y. Chujo, Langmuir 22 (2006) 7760.
[8] H. Cölfen, Curr. Opin. Colloid Interface Sci. 8 (2003) 23.
[9] S. Mann, J.M. Didymus, N.P. Sanderson, B.R. Heywood, E.J.A. Samper, J. Chem. Soc. Faraday Trans. 86 (1990) 1873.
[10] D.B. DeOliveira, R.A. Laursen, J. Am. Chem. Soc. 119 (1997) 10627.
[11] F.C. Meldrum, S.T. Hyde, J. Crystal Growth 231 (2001) 544.
[12] S.H. Yu, H. Cölfen, M. Antonietti, J. Phys. Chem. B 17 (2003) 7396.
[13] J.J.J.M. Donners, B.R. Heywood, E.W. Meijer, R.J.M. Nolte, N.A.J.M. Sommerdijk, Chem. Eur. J. 8 (2002) 2561.
[14] L.B. Gower, D.J. Odom, J. Crystal Growth 210 (2000) 719.
[15] S. Raz, S. Weiner, L. Addadi, Adv. Mater. 12 (2000) 38.
[16] S. Weiner, L. Addadi, J. Mater. Chem. 7 (1997) 689.
[17] J. Aizenberg, J. Hanson, T.F. Koetzle, S. Weiner, L. Addadi, J. Am. Chem. Soc. 119 (1997) 881.
[18] T. Kato, A. Sugawara, N. Hosoda, Adv. Mater. 14 (2002) 869.
[19] A.-W. Xu, Y. Ma, H. Cölfen, J. Mater. Chem. 17 (2007) 415.
[20] E. Ruiz-Hitzky, M. Darder, P. Aranda, in: E. Ruiz-Hitzky, K. Ariga, Y. Lvov (Eds.), Bio-Inorganic Hybrid Materials, Wiley-VCH, Weinheim, 2007 Chapter 1.
[21] M. Darder, P. Aranda, E. Ruiz-Hitzky, Adv. Mater. 19 (2007) 1309.
[22] F.C. Meldrum, Int. Mater. Rev. 48 (2003) 187.
[23] C.M. Zaremba, A.M. Belcher, M. Fritz, Y.L. Li, S. Mann, P.K. Hansma, D.E. Morse, J.S. Speck, G.D. Stucky, Chem. Mater. 8 (1996) 679.
[24] S. Weiner, W. Traub, Philos. Trans. R. Soc. London B 304 (1984) 425.
[25] M. Rinaudo, Prog. Polym. Sci. 31 (2006) 603.
[26] M.E. Marsh, in: E. Baeuerline (Ed.), Biomineralization: From Biology to Biotechnology and Medical Applications, Wiley-VCH, Weinheim, 2000, p. 251.
[27] J.M. Didymus, P. Oliver, S. Mann, A.L. DeVries, P.V. Hauschka, P. Westbroek, J. Chem. Soc. Faraday Trans. 89 (1993) 2891.
[28] E. Doncel-Pérez, M. Darder, E. Martín-López, L. Vázquez, M. Nieto-Sampedro, E. Ruiz-Hitzky, J. Mater. Sci. Mater. Med. 17 (2006) 795.
[29] G. Falini, S. Fermani, M. Gazzano, A. Ripamonti, Chem. Eur. J. 4 (1998) 1048.
[30] M. Chaplin, 〈http://www.lsbu.ac.uk/water/hycar.html〉, last update on 24 May, 2008.
[31] J.H. Huang, Z.F. Mao, M.F. Luo, Mater. Res. Bull. 42 (2007) 2184.
[32] M. Suzuki, H. Nagasawa, T. Kogure, Cryst. Growth Des. 6 (2006) 200.
[33] A. Neira-Carrillo, M. Yazdani-Pedram, J. Retuert, M. Diaz-Dosque, S. Gallois, J.L. Arias, J. Colloid Interface Sci. 286 (2005) 134.
[34] S. Fuentes, J. Retuert, G. González, E. Ruiz-Hitzky, Int. J. Polym. Mater. 35 (1997) 61.
[35] C.A. Orme, A. Noy, A. Wierzbicki, M.T. McBride, M. Grantham, H.H. Teng, P.M. Dove, J.J. DeYoreo, Nature 411 (2001) 775.
[36] L. Addadi, S. Raz, S. Weiner, Adv. Mater. 15 (2003) 959.
[37] H. Fabritius, A. Ziegler, J. Struct. Biol. 142 (2003) 281.
[38] J.W. Morse, R.S. Arvinson, A. Lüttge, Chem. Rev. 107 (2007) 342.
[39] J.L. Arias, A. Neira-Carrillo, J.I. Arias, C. Escobar, M. Bodero, M. David, M.S. Fernandez, J. Mater. Chem. 14 (2004) 2154.
[40] J. Aizenberg, A.J. Black, G.M. Whitesides, J. Am. Chem. Soc. 121 (1999) 4500.
[41] S. Mann, B.R. Heywood, S. Rajam, J.D. Birchall, Nature 334 (1988) 692.
[42] J. Aizenberg, A.J. Black, G.M. Whitesides, Nature 398 (1999) 495.
[43] N. Jongen, P. Bowen, J. Lemaître, J.-C. Valmalette, H. Hofmann, J. Colloid Interface Sci. 226 (2000) 189.
[44] S. Albeck, J. Aizenberg, L. Addadi, S. Weiner, J. Am. Chem. Soc. 115 (1993) 11691.
[45] J. Aizenberg, M. Ilan, S. Weiner, L. Addadi, Connect. Tissue Res. 34 (1996) 255.
[46] S. Albeck, L. Addadi, S. Weiner, Connect. Tissue Res. 35 (1996) 419.
[47] S. Albeck, S. Weiner, L. Addadi, Chem. Eur. J. 2 (1996) 278.
[48] J. Aizenberg, J. Hanson, T.F. Koetzle, S. Weiner, L. Addadi, J. Am. Chem. Soc. 119 (1997) 881.